Renewable-Resource Thermoplastic Elastomers Based on Polylactide and Polymenthide

Carolyn L. Wanamaker, Leslie E. O'Leary, Nathaniel A. Lynd, Marc A. Hillmyer,* and William B. Tolman*

Department of Chemistry, University of Minnesota, 207 Pleasant Street SE, Minneapolis, Minnesota 55455-0431

Received June 22, 2007; Revised Manuscript Received September 13, 2007

An α,ω-functionalized polymenthide was synthesized by the ring-opening polymerization of menthide in the presence of diethylene glycol with diethyl zinc as the catalyst. Termination with water afforded the dihydroxy polymenthide. The reaction of this telechelic polymer with triethylaluminum formed the corresponding aluminum alkoxide macroinitiator that was used for the controlled polymerization of lactide to yield biorenewable polylactide-*b*-polymenthide-*b*-polylactide triblock copolymers. The molecular weight and chemical composition were easily adjusted by the monomer-to-initiator ratios. Microphase separation in these triblock copolymers was confirmed by small-angle X-ray scattering and differential scanning calorimetry. A representative triblock was prepared with a hexagonally packed cylindrical morphology as determined by small-angle X-ray scattering, and tensile testing was employed to assess the mechanical behavior. On the basis of the ultimate elongations and elastic recovery, these triblock copolymers behaved as thermoplastic elastomers.

Introduction

Polylactide is an attractive biodegradable polyester that possesses many desirable properties such as nontoxicity, hydrolyzability, and biocompatibility.[1] These properties contribute to polylactide's potential for use in the biomedical and pharmaceutical fields.[2,3] Polylactide is most commonly synthesized by the ring-opening polymerization of lactide, the cyclic dimer of lactic acid.[4] Polymerization of racemic D,L-lactide typically results in atactic, amorphous ($T_g \approx 60$ °C) poly(D,L-lactide) (PLA), whereas polymerization of L-lactide or D-lactide results in isotactic, semicrystalline ($T_m \approx 180$ °C) poly(L-lactide) (PLLA) or poly(D-lactide) (PDLA).[5] Under tension, polylactide fractures at very low strains (ca. 3%), and is therefore unsuitable for use in numerous applications where elasticity and ductility are essential. Modifications of polylactide by plasticization,[6] blending,[7] and incorporation into block copolymers[8] can be used to enhance its portfolio of properties, thus widening its applicability.

With the aim of enhancing the utility of polylactide, we have been interested in polylactide-containing ABA triblock copolymers. ABA triblock copolymers that contain immiscible segments where A is a "hard", high T_g or semicrystalline polymer and B is a "soft" amorphous, low T_g polymer can behave as thermoplastic elastomers (TPEs).[9] The mechanical properties of this class of triblock copolymer are a result of the microphase separation of the soft and hard blocks in which the soft, rubbery matrix phase is physically cross-linked by the microphase-separated hard phase, thus providing both strength and elasticity.[9,10] The stress−strain properties of TPEs are similar to that of vulcanized rubbers, but the materials can be processed like conventional thermoplastics.[9]

Polylactide-containing ABA triblock copolymers with non-biodegradable, non-renewable midblocks, such as polyisoprene (PI),[11,12] an aniline pentamer,[13] and polyisobutylene,[14] have been synthesized. We have shown that PLA-*b*-PI-*b*-PLA triblock copolymers exhibited high elongations (especially for a sample with cylindrical morphology, with ultimate elongations of 650 ± 70%) and good elastomeric recovery, but this system has drawbacks because it is inherently only partially renewable and biodegradable.[11] The synthesis of fully biodegradable triblock copolymer systems containing a poly(3-hydroxybutyrate) (PHB), poly(1,3-trimethylene carbonate) (PTMC), poly(1,5-dioxepan-2-one), poly(ϵ-caprolactone), or poly(ethylene oxide) middle blocks and PLA, PLLA, or PDLA end blocks has also been investigated.[15−18] The triblock copolymer series PLLA-*b*-PHB-*b*-PLLA showed an improved initial modulus relative to the elastomeric homopolymer PHB, but demonstrated low ultimate elongations of less than 200%.[15] The triblock copolymers PLLA-*b*-PTMC-*b*-PLLA and PDLA-*b*-PTMC-*b*-PDLA exhibited impressive elongations of >1800% when containing 10 mol % PLLA or PDLA, and low creep rates were obtained by stereocomplex formation between enantiomeric polylactide segments of the triblock copolymers in blends.[16]

Such completely biodegradable ABA triblock copolymers as those described above will expand the potential utility of TPEs to be used in applications such as drug delivery matrices, flexible implants, substrates for cell culture and scaffolds for tissue engineering.[2,19] We are interested in using polymenthide (PM)[20] as the soft, low T_g segment of a PLA containing ABA triblock copolymer. PM is one of a variety of new polymers derived from biorenewable resources.[21] The ring-opening polymerization of menthide (**M**, Scheme 1), a derivative of (−)-menthol, was investigated by Zhang et al.,[20] who showed that **M** can be polymerized in a controlled fashion with molecular weights up to 91 kg/mol. PM is a noncrystalline, amorphous polymer that exhibits a T_g of −25 °C, making it a suitable candidate for a soft segment in TPEs. We have found that PM and PLA homopolymers are immiscible (at moderate molecular weight, a blend of PM (30 kg/mol) and PLA (30 kg/mol) exhibits two glass transition temperatures corresponding to each of the

* To whom correspondence should be addressed. E-mail: hillmyer@chem.umn.edu (M.A.H.); tolman@chem.umn.edu (W.B.T.).

10.1021/bm700699g CCC: $37.00
Published on Web 10/26/2007

Scheme 1

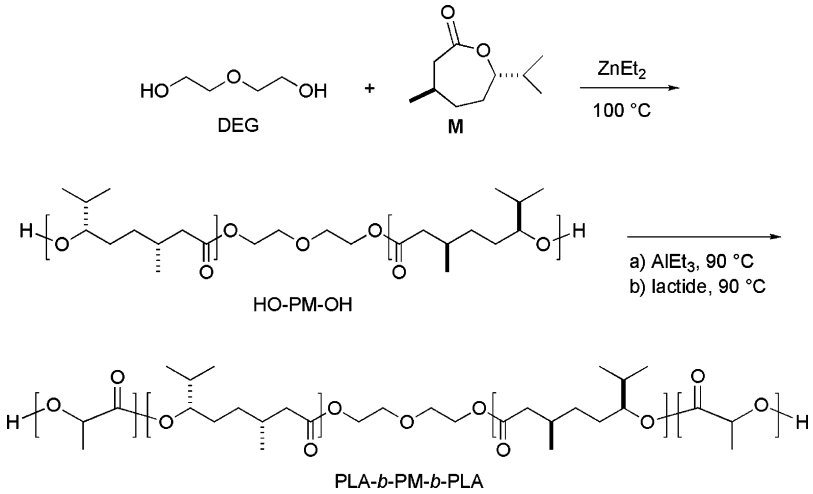

homopolymers) and have the potential to microphase separate once incorporated in block copolymers. We herein report the synthesis of PLA-*b*-PM-*b*-PLA TPEs and their full characterization, including by ^{1}H and ^{13}C NMR spectroscopy, size exclusion chromatography (SEC), differential scanning calorimetry (DSC), and small-angle X-ray scattering (SAXS). We also synthesized a PLA-*b*-PM-*b*-PLA triblock copolymer on a 2 g scale for mechanical testing, the results of which demonstrated its elastomeric behavior.

Experimental Section

Materials. All air- or moisture-sensitive compounds were handled under a nitrogen atmosphere in a glovebox, as indicated. Toluene used for polymerizations was purified by passing through activated alumina-based columns (Glass Contour, Laguna Beach, CA) followed by distillation from sodium. D,L-Lactide (Purac) was purified by recrystallization from toluene followed by repeated (2×) vacuum sublimation. Diethylene glycol (DEG; Sigma Aldrich) was distilled under reduced pressure from sodium. Molecular sieves (4 Å) were dried under vacuum at 180 °C for a minimum of 16 h. All other solvents and reagents were used as received from the commercial source indicated without further purification. All glassware used in polymerizations was treated with a solution of Me_2SiCl_2 (10% in CH_2Cl_2) and oven dried at 200 °C for a minimum of 3 h before use.

Measurements. ^{1}H and ^{13}C NMR spectra were collected on a Varian INOVA-300, VXR-300 or Varian INOVA-500 spectrometer. Samples of the polymers were prepared by dissolving approximately 30 mg of polymer in 1 mL of $CDCl_3$ (Cambridge). Molecular weights (M_n and M_w) and polydispersity indices (PDIs) (M_w/M_n) were determined by SEC using polystyrene standards. Samples were analyzed at 40 °C using a Hewlett-Packard high-pressure liquid chromatograph equipped with three Jordi poly(divinylbenzene) columns of 10^4, 10^3, and 500 Å pore sizes and a HP1047A differential refractometer. Fourier transform infrared (FT-IR) spectra were collected on a Thermo Nicolet Avatar 370 FT-IR spectrometer. The kinetics of selected polymerizations were monitored by a Mettler Toledo ReactIR 4000 equipped with a diamond probe. DSC measurements were performed using a TA Instruments Q1000 with nitrogen as the purge gas. An indium standard was used for calibration, and the scan rate was 10 °C/min. Samples weighing 3.0−8.0 mg were loaded into aluminum hermetic pans, and the pans were sealed prior to measurement. Measurements for SAXS were performed at the University of Minnesota Twin Cities Characterization Facility beamline. Cu Kα X-rays (λ = 1.542 Å) were generated by a Rigaku RU-200BVH rotating anode fitted with a 0.2 × 2 mm^2 microfocus cathode and Franks mirror optics. Temperature control inside the evacuated sample chamber was accomplished with water-cooling and electrically heating the brass-block sample holder. All samples were heated to 160 °C and annealed for 10 min in the sample chamber prior to SAXS measurements at 80−160 °C. Two-dimensional diffraction images were recorded using a Siemens area detector located at the end of a 2.30 m evacuated flight tube and corrected for detector response before analysis. The two-dimensional images were azimuthally integrated and reduced to the one-dimensional form of scattered intensity versus the spatial frequency q. Tensile deformation experiments were carried out at room temperature using a Rheometrics Scientific Minimat instrument operated at a cross-head speed of 5 mm/min. The sample gage length was 5 mm, the gage width was 3 mm, and the gage thickness was 1 mm.

General Procedure for the Synthesis of PM. As previously reported,[20] **M** was synthesized from (−)-menthone using *meta*-chloroperbenzoic acid.[22] **M** was readily obtained on a 100 g scale in >70% yield by recrystallization from hexanes and sublimation of the crude product. Initial monomer concentrations were kept at 1 M. A stock solution of DEG ([DEG] = 0.10 M in tetrahydrofuran (THF)) was stored in the glovebox at −30 °C. The amount of catalyst and DEG used varied depending on the desired molecular weight of the resulting polymers. A representative procedure was as follows: In the glovebox, portion of DEG solution (1.84 mL, 0.184 mmol) was injected into the reaction flask followed by the addition of diethyl zinc ($ZnEt_2$; Sigma Aldrich, 1.0 M in hexanes) (918 μL, 0.918 mmol). The reaction flask was then charged with **M** (2.500 g, 14.68 mmol), toluene (11.93 mL), and a stir bar. The reaction flask was sealed and taken out of the glovebox to stir at 100 °C for 4.5 h (73% conversion of monomer). Exposure to air and the addition of water (3.0 mL) quenched the reaction. The majority of the solvent was evaporated, and the polymer was washed with methanol at 0 °C and dried at 90 °C in a vacuum oven (1.7 g recovered, 93% yield). ^{1}H NMR ($CDCl_3$) δ 4.73 (m, 161H), 4.23 (t, J = 4.5 Hz, 4H), 3.69 (t, J = 4.5 Hz, 4H), 3.34 (m, 1H), 2.30 (dd, J_{AB} = 15.3 Hz, J = 5.4 Hz, 161H), 2.07 (dd, J_{AB} = 14.4 Hz, J = 8.4 Hz, 161H), 1.94 (m, 161H), 1.82 (m, 161H), 1.53 (m, 322H), 1.33 (m, 161H), 1.18 (m, 161H), 0.94 (d, J = 6.6 Hz, 482H), 0.89 (d, J = 6.9 Hz, 964H); ^{13}C{^{1}H} NMR ($CDCl_3$) δ 173.2, 78.6, 42.2, 32.9, 31.4, 30.6, 28.7, 20.0, 18.9, 17.7.

General Procedure for the Synthesis of LML Triblock Copolymers. Initial D,L-lactide concentrations were kept at 1.0 M. The amount of D,L-lactide used varied depending on the molecular weight of the macroinitiator. Each macroinitiator copolymerization series was performed under identical initial conditions (exception: LML(3.3−28−3.3)). The time allowed for each block copolymerization in the series was tailored to the product molecular weights desired. A typical procedure was as follows: In the glovebox, a reaction flask was charged with PM10 (Table 1, 0.1250 g, 0.0125 mmol) and toluene (0.988 mL) followed by the addition of $AlEt_3$ (Sigma Aldrich, 1.0 M in heptane) (12.5 μL, 0.0125 mmol). The reaction flask was sealed and removed

Table 1. Data for Ring-Opening Polymerization of **M**[a]

sample	$[\mathbf{M}]_0/[DEG]_0$	conv[b] (%)	time (h)	M_n[b] (conv) (kg/mol)	M_n[b] (EG) (kg/mol)	M_n (SEC) (kg/mol)	PDI (SEC)	F_n[c] (NMR)	T_g[d] (°C)
PM10	80	73	4.5	9.9	10	20	1.28	2.4	−26
PM28	220	76	7.0	28	29	35	1.31	2.6	−26
PM43	310	81	10.3	43	38	55	1.28	2.7	−25

[a] Conditions: $[\mathbf{M}]_0 = 1.0$ M, $[Zn]_0 = 0.063$ M (PM10); 0.023 M (PM28); 0.016 M (PM43), toluene, 100 °C, $[\mathbf{M}]_{eq} = 0.120 \pm 0.063$ M.[20] [b] Calculated from ^{1}H NMR spectroscopy. [c] Calculated from relative integrations of HO−PM−OH end groups and DEG in the ^{1}H NMR spectrum. [d] Determined by DSC.

from the glovebox to stir at 90 °C. After 30 min, the reaction flask was brought into the glovebox, and D,L-lactide (0.144 g, 1.00 mmol) was added. The resultant mixture was heated at 90 °C with stirring outside the glovebox for 50 min (41% conversion of monomer). The reaction flask was then exposed to air, and 10% HCl solution was added (3.0 mL) to quench the reaction. Minimal toluene was added (ca. 1 mL), and the organic layer was precipitated into an excess of methanol at 0 °C (300 mL). The product was isolated and dried in a vacuum oven at 80 °C overnight (70% yield assuming complete recovery of the PM block). ^{1}H NMR ($CDCl_3$) δ 5.19 (m, 66H), 4.73 (m, 161H), 4.23 (t, $J = 4.5$ Hz, 4H), 3.69 (t, $J = 4.2$ Hz, 4H), 2.30 (dd, $J_{AB} = 14.4$ Hz, $J = 5.4$ Hz, 161H), 2.08 (dd, $J_{AB} = 14.7$ Hz, $J = 8.7$ Hz, 161H), 1.94 (m, 161H), 1.82 (m, 161H), 1.60 (m, 196H), 1.53 (m, 322H), 1.33 (m, 161H), 1.18 (m, 161H), 0.94 (d, $J = 6.3$ Hz, 482H), 0.89 (d, $J = 6.6$ Hz, 964H); $^{13}C\{^1H\}$ NMR ($CDCl_3$) δ 173.1, 169.3, 78.4, 69.2, 42.1, 32.8, 31.3, 30.5, 28.6, 19.9, 18.8, 17.7, 16.8.

Kinetic Experiments. A ReactIR 4000 spectrometer was used to monitor the polymerization reactions in situ. The glassware used was oven dried at 200 °C for at least 3 h. The ReactIR probe and the reaction flask containing a solution of monomer, catalyst, and initiator were assembled in the glovebox and quickly attached to the spectrometer outside the glovebox. The consumption of **M** was monitored to over 5 half-lives at 1274 and 1048 cm^{-1}. A nonlinear fit of the curve to $A_t = (A_o - A_\infty) \exp(-k_{obs}t) + A_\infty$ gave the observed rate constant (k_{obs}). On the basis of previous kinetic experiments, the dependence on $[ZnEt_2]$ was assumed to be first-order.[20,24] The second-order rate constant, k_p, was therefore calculated by using the equation $k_{obs} = k_p[ZnEt_2]_0$.

Synthesis of PM29. In the glovebox, a volume of 0.10 M DEG (1.60 mL, 0.160 mmol) was injected into a reaction flask followed by the addition of $ZnEt_2$ (801 μL, 0.801 mmol). The reaction flask was then charged with **M** (6.00 g, 35.2 mmol) and toluene (32.84 mL), and a stir bar was added. The reaction flask was sealed and taken out of the glovebox to stir at 100 °C for 5.25 h. Exposure to air and the addition of 10% HCl solution (ca. 20 mL) quenched the reaction. The solution was shaken, and the emulsion was precipitated into an excess of −78 °C methanol (ca. 300 mL). The polymer was isolated, dissolved in minimal CH_2Cl_2, and precipitated into a second flask of −78 °C methanol (ca. 300 mL). The second isolation was performed, and the majority of the solvent was evaporated under a stream of N_2. The product was dried at 40 °C in a vacuum oven overnight (70% yield). SEC (THF) $M_n = 21.1$ kg/mol, $M_w = 26.7$ kg/mol, $M_n/M_w = 1.26$; M_n (^{1}H NMR) = 29.4 kg/mol; ^{1}H NMR ($CDCl_3$) δ 4.73 (m, 170H), 4.23 (t, $J = 4.5$ Hz, 4H), 3.69 (t, $J = 4.5$ Hz, 4H), 3.34 (m, 1H), 2.30 (dd, $J_{AB} = 15.3$ Hz, $J = 5.4$ Hz, 170H), 2.07 (dd, $J_{AB} = 14.4$ Hz, $J = 8.4$ Hz, 170H), 1.94 (m, 170H), 1.82 (m, 170H), 1.53 (m, 340H), 1.33 (m, 170H), 1.18 (m, 170H), 0.94 (d, $J = 6.6$ Hz, 510H), 0.89 (d, $J = 6.9$ Hz, 1020H); $^{13}C\{^1H\}$ NMR ($CDCl_3$) δ 173.2, 78.6, 42.2, 32.9, 31.4, 30.6, 28.7, 20.0, 18.9, 17.7.

Synthesis of the LML(7.8−29−7.8) Triblock Copolymer. In the glovebox, a reaction flask was charged with PM29 (Table 1, 1.50 g, 0.0510 mmol), toluene (5.15 mL), and molecular sieves and allowed to stir overnight. $AlEt_3$ (0.0510 mL, 0.0510 mmol) was added to the reaction flask, which was sealed and removed from the glovebox to stir at 90 °C. After 30 min, D,L-lactide (0.750 g, 5.20 mmol) was added to the reaction flask in the glovebox. The resultant mixture was heated at 90 °C with stirring for 4.5 h. The reaction flask was then exposed to air, and 10% HCl solution was added (ca. 6 mL) to quench the reaction. Minimal toluene was added (ca. 1 mL), and the solution was shaken and precipitated into an excess of −78 °C methanol (ca. 300 mL). The polymer was isolated and precipitated into a second flask of −78 °C methanol (ca. 300 mL). The resulting polymer was dissolved in minimal dichloromethane and filtered to remove the molecular sieves. The product was dried in a vacuum oven at 50 °C overnight (75% yield assuming complete recovery of the PM block). SEC (THF) $M_n = 29.5$ kg/mol, $M_w = 36.9$ kg/mol, $M_n/M_w = 1.25$; M_n (^{1}H NMR) = 45.0 kg/mol; ^{1}H NMR ($CDCl_3$) δ 5.19 (m, 108H), 4.73 (m, 170H), 4.23 (t, $J = 4.5$ Hz, 4H), 3.69 (t, $J = 4.2$ Hz, 4H), 2.30 (dd, $J_{AB} = 14.4$ Hz, $J = 5.4$ Hz, 1H), 2.08 (dd, $J_{AB} = 14.7$ Hz, $J = 8.7$ Hz, 170H), 1.94 (m, 170H), 1.82 (m, 170H), 1.60 (m, 324H), 1.53 (m, 340H), 1.33 (m, 170H), 1.18 (m, 170H), 0.94 (d, $J = 6.3$ Hz, 510H), 0.89 (d, $J = 6.6$ Hz, 1020H); $^{13}C\{^1H\}$ NMR ($CDCl_3$) δ 173.1, 169.3, 78.4, 69.2, 42.1, 32.8, 31.3, 30.5, 28.6, 19.9, 18.8, 17.7, 16.8.

Results and Discussion

Preparation of HO−PM−OH. As shown in Scheme 1, difunctional PM (HO−PM−OH) was prepared using the difunctional initiator DEG. $ZnEt_2$ was used as the catalyst due to its availability and low cost.[23] To guarantee the polymerization of **M**, a $[ZnEt_2]/[OH]$ ratio of 2.5 was employed. All polymerizations of **M** were performed at 100 °C in toluene ($[\mathbf{M}]_0 = 1.0$ M) under an inert atmosphere.

The rate of polymerization of **M** using DEG and $ZnEt_2$ was determined by monitoring the decay of the absorbance of the peaks at 1274 and 1048 cm^{-1} by in situ FT-IR spectroscopy. The decay of [**M**] over time was found to be exponential, characteristic of first-order dependence on [**M**]. On the basis of a previous kinetic experiment, the dependence on $[ZnEt_2]$ was assumed to be first-order.[20,24] The propagation rate constant k_p for varied $ZnEt_2$ loadings was $(3.5 \pm 0.35) \times 10^{-3}$ M^{-1} s^{-1} at 100 °C (Figure S1). At a typical concentration of $[ZnEt_2]_0$ of 0.023 M, the half-life for this polymerization is about 140 min.

The molecular weights of HO−PM−OH could be controlled by varying the monomer-to-initiator ratios and controlling the conversion of **M** (Table 1). Polymerizations were quenched by exposure to air and water at approximately 75% conversion of **M** (confirmed by NMR spectroscopy). The molecular weights (by SEC versus polystyrene standards) of HO−PM−OH were generally controlled, as demonstrated by the increase in the apparent molecular weight of HO−PM−OH with the decrease of DEG in the feed and by the linear increase in molecular weight and $([\mathbf{M}]_0 - [\mathbf{M}]_t)/[I]_0$ with a *y*-intercept near zero. The PDIs for HO−PM−OH obtained by this method were relatively narrow (PDI $\approx$ 1.3).

^{1}H NMR spectroscopy was employed to verify end functionalization, confirm the connectivity of DEG in the polymer chain, and determine the M_n. All proton signals of the PM repeating units agree with those found in the previous literature.[20] Figure 1a shows the typical expanded ^{1}H NMR spectrum from δ 3.0−4.4 ppm of the difunctional PM. The two methylene resonances attributed to the internal DEG unit appear at δ 3.68 ppm (H_a) and 4.22 ppm (H_b), and the resonance of the methine protons α to the hydroxyl chain end is apparent at δ 3.35 ppm (H_c).

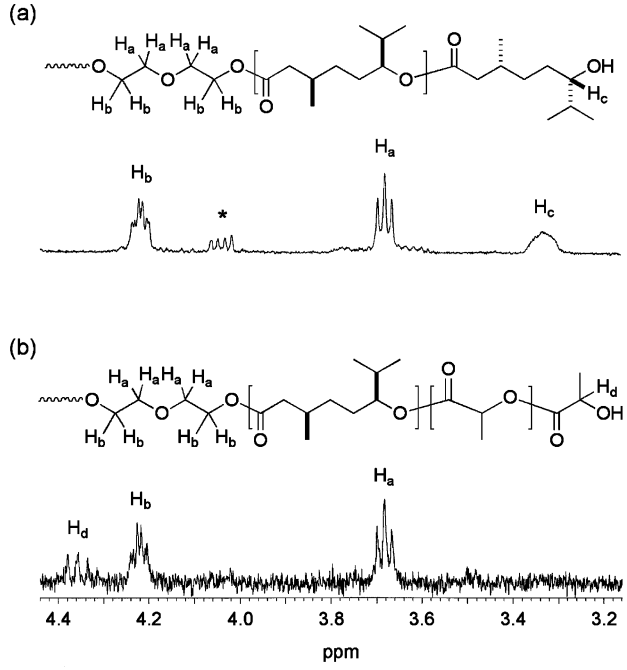

Figure 1. Expanded ^{1}H NMR spectra for (a) HO−PM−OH (* = methine proton of residual **M**) and (b) PLA-*b*-PM-*b*-PLA.

The resonance from the HO−PM−OH methine protons α to the hydroxyl chain end (Figure 1a, H_c) was used to determine the M_n of the polymer chain (assuming exactly two end groups per chain). The M_n values were calculated from the integral ratio of these protons relative to the main chain methine resonance at δ 4.70 ppm. We observed excellent agreement between the calculated M_n and the M_n based on the conversion of the monomer (Table 1), confirming the average chain end functionality (F_n) to be 2. We observed a ratio of 1:1 when comparing the resonances of the protons on the DEG unit (Figure 1a, H_a and H_b). However, the integration ratio of the HO−PM−OH terminal methine protons (Figure 1, H_c) to the resonance from the protons on the DEG unit (Figure 1, H_a and H_b), gave F_n values greater than 2 (Table 1). On the basis of these high F_n values, we conclude that there is an inconsistency between the number of DEG units expected in the polymer chain and the number of DEG units observed, while the observed number of terminal methine protons (Figure 1, H_c) per polymer chain is as expected (because of the agreement between the calculated M_n based on the integration of the terminal methine protons and the M_n based on conversion of the monomer). We are not certain as to why this inconsistency in the number of DEG units per polymer chain exists. $^{13}C\{^1H\}$ NMR and IR spectroscopic data for the HO−PM−OH samples were consistent with previous data reported,[20] and DSC revealed T_g's of the PM samples of about −25 °C. No crystallinity was detected up to 100 °C.

Synthesis and Characterization of PLA-*b*-PM-*b*-PLA Triblock Copolymers. The set of HO−PM−OH samples given in Table 1 were used as macroinitiators in the metal-catalyzed ring-opening polymerization of lactide. Aluminum alkoxides formed from $AlEt_3$ and HO−PM−OH were targeted as the initiators. To avoid the formation of gels, $[OH]_0/[Al]_0 = 2$ was chosen.[11] All polymerizations were performed at 90 °C and quenched by exposure to air and dilute HCl. A linear increase in molecular weight with $([LA]_0 - [LA]_t)/[I]_0$ was observed with a *y*-intercept near zero, consistent with the controlled polymerization of lactide. Triblock copolymers containing 20, 30, 40, and 50% PLA by mass were targeted. These series of triblock copolymers are summarized in Table 2.

The PLA-*b*-PM-*b*-PLA triblock copolymers were characterized by ^{1}H NMR spectroscopy. The percent conversion of D,L-lactide in solution was measured by integration of the resonance from the methine protons corresponding to the polylactide chain (δ 5.18 ppm) and the resonance from the methine protons corresponding to D,L-lactide (δ 5.05 ppm). The resonance for the methine protons α to the hydroxyl functionality at the chain ends of HO−PM−OH (δ 3.35 ppm) was absent in the PLA-*b*-PM-*b*-PLA triblock copolymers (Figure 1b). This resonance was replaced by the resonance of the methine protons of the chain ends of the triblock copolymers (δ 4.36 ppm). Last, ^{1}H NMR spectroscopy was used to determine the percent PLA in the triblock copolymer by comparing the resonance from the methine protons corresponding to the PLA blocks and the resonance from the methine protons corresponding to the PM block. We observed excellent agreement between the calculated percent PLA based on the conversion of monomer in solution and the determined percent PLA in the product.

Triblock copolymer formation was detected by the shift of the SEC traces relative to the respective homopolymer traces; a representative series is given in Figure 2. As the PLA composition increases for each series of triblock copolymers, a shift toward the high molecular weight occurs. The molecular weight distributions of the triblock copolymers were relatively narrow (PDI = 1.2−1.4).

Thermal Properties and Morphology of PLA-*b*-PM-*b*-PLA Triblock Copolymers. Microphase separation of the PLA-*b*-PM-*b*-PLA triblock copolymers is necessary to achieve the physical properties associated with TPEs.[9] DSC and SAXS characterization were used to determine the immiscibility and ordered morphology of the triblock copolymers, respectively. DSC analysis of all triblock copolymers revealed two glass transition temperatures, consistent with microphase separation (Table 3). For each series, the T_g values corresponding to the PM blocks were relatively invariant (ca. −22 °C), while the T_g values corresponding to the PLA blocks range from 20 to 51 °C depending on the molecular weight of the PLA block. Figure 3 shows representative DSC thermograms of the PM28 triblock copolymer series.

SAXS of PLA-*b*-PM-*b*-PLA Triblock Copolymers. SAXS was used to examine the spatial distribution of microphase-separated domains in these PLA-*b*-PM-*b*-PLA triblock copolymers. Figure 4 shows the SAXS results for each sample at 80 °C. All of the PLA-*b*-PM-*b*-PLA triblock copolymers exhibited a principal reflection, **q***, followed by several higher-order reflections (Figure 4b,c,f). In some samples, broad oscillations in intensity (Figure 4e,g,h,i,j,k) followed the principal reflection consistent with microphase-separated domains that do not exhibit long-range order. On the basis of the positions of the higher order reflections, lamellar morphologies were observed for LML(4.6−10−4.6) and LML(14−28−14), and hexagonal morphologies were observed for LML(2.3−10−2.3), LML(3.8−10−3.8), and LML(6.6−28−6.6). We could not definitively determine the exact nature of the microphase-separated domains for the balance of the triblock copolymers and denote them as micellar (Table 3). On the basis of the SAXS data for three of the triblock copolymers in the lowest molecular weight series (Figure 4b,c,d), we suspect that the higher molecular weights of the samples shown in Figures 4e−h kinetically thwart the attainment of long-range order.

A crude estimate of the effective interaction parameter between PLA and PM was made based on the change in lamellar

Table 2. Results of the Block Copolymerization of D,L-lactide Initiated with Dihydroxyl-Terminated PM[a]

triblock	$[LA]_0/[PM]_0$	LA conv[b] (%)	time (min)	PLA−PM−PLA M_n (NMR) (kg/mol)	% PLA[c]	M_n (SEC) (kg/mol)	PDI (SEC)	yield[d] (%)
LML (1.3−10−1.3)	80	21	20	1.3−9.9−1.3	20.2	24.0	1.22	65
LML (2.3−10−2.3)	80	41	50	2.3−9.9−2.3	31.6	29.9	1.19	70
LML (3.8−10−3.8)	80	58	60	3.8−9.9−3.8	42.8	32.2	1.22	69
LML (4.6−10−4.6)	80	79	100	4.6−9.9−4.6	48.0	35.5	1.22	54
LML (3.3−28−3.3)	62	79	60	3.3−28-3.3	18.9	48.0	1.29	66
LML (6.6−28−6.6)	220	38	45	6.6−28-6.6	31.8	54.1	1.28	75
LML (9.7−28−9.7)	220	66	90	9.7−28-9.7	40.7	50.5	1.40	53
LML (14−28−14)	220	86	120	14−28-14	49.9	66.9	1.34	86
LML (6.5−43−6.5)	400	19	35	6.5−43-6.5	23.1	64.1	1.29	89
LML (10−43−10)	400	33	60	10−43-10	32.1	71.2	1.30	75
LML (15−43−15)	400	54	60	15−43-15	41.2	69.8	1.39	84
LML (23−43−23)	400	74	85	23−43-23	51.5	90.8	1.41	75

[a] Conditions: $[LA]_0 = 1.0$ M, toluene, 90 °C. [b] Calculated from ^{1}H NMR spectroscopy. [c] Mass percent PLA calculated from ^{1}H NMR spectroscopy and composition of the triblock copolymers. [d] Isolated yield.

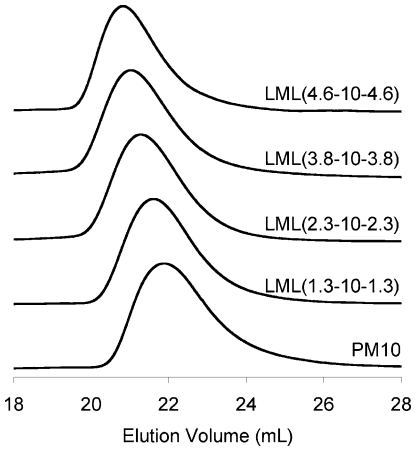

Figure 2. SEC data for PM10 and the corresponding triblock copolymers.

Table 3. Thermal and Morphological Properties of PLA-*b*-PM-*b*-PLA Triblock Copolymers

triblock	% PLA[a]	morphology[b]	D (Å)[c]	$T_{g(PM)}$[d] (°C)	$T_{g(PLA)}$[d] (°C)
LML(1.3−10−1.3)	20.2	disordered	135	−22	21
LML(2.3−10−2.3)	31.6	cylindrical	178	−22	38
LML(3.8−10−3.8)	42.8	cylindrical	209	−22	42
LML(4.6−10−4.6)	48.0	lamellar	194	−21	44
LML(3.3−28−3.3)	18.9	micellar[e]	231	−22	34
LML(6.6−28−6.6)	31.8	cylindrical	259	−22	46
LML(9.7−28−9.7)	40.7	micellar[e]	471	−22	46
LML(14−28−14)	49.9	lamellar	367	−22	50
LML(6.5−43−6.5)	23.1			−22	48
LML(10−43−10)	32.1	micellar[e]	314	−21	51
LML(15−43−15)	41.2	micellar[e]	357	−21	53
LML(23−43−23)	51.5	micellar[e]	455	−22	53

[a] Mass percent PLA calculated from ^{1}H NMR spectroscopy and composition of the triblock copolymers. [b] Based on SAXS data from 80 to 160 °C. [c] Determined by SAXS from the primary reflection ($D = 2\pi/\mathbf{q}^*$) at 80 °C. [d] Determined by DSC. [e] The SAXS data of these samples consist of a strong primary reflection followed by several low-amplitude, broad peaks due to the form of the microphase-separated domains.

domain spacing of LML(4.6−10−4.6) as a function of temperature. Equation 1 describes the domain spacing of strongly segregated lamellar mesostructures:[25]

$$D = 1.10bN^{2/3}\chi^{1/6} \quad (1)$$

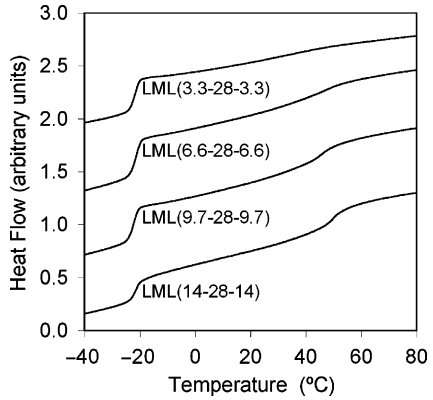

Figure 3. DSC analysis data for LML(3.3−28−3.3), LML(6.6−28−6.6), LML(9.7−28−9.7), and LML(14−28−14).

where b is the statistical segment length, N is the number of segments, and χ is the effective interaction parameter and is customarily given the functional form $\chi = A/T + B$. For simplicity, the average statistical segment length was assumed to be 8 Å, and N is equal to the overall degree of polymerization. Figure 5 depicts the measured lamellar domain spacing ($D = 2\pi/\mathbf{q}^*$) divided by $1.10bN^{2/3}$ and raised to the sixth power versus inverse temperature. The line-of-best-fit represents the estimate of χ. The effective interaction parameter that results from this analysis for this compositionally symmetric triblock copolymer is $\chi = 364/T - 0.50$. Our assumptions for b and N amount to using an unknown segment reference volume for each. χ represents interaction per segment volume, so meaningful comparison with χ for other block copolymer systems cannot be made. However, we feel this analysis gives a reasonable estimate of χ between PM and PLA.

Mechanical Properties for PLA-*b*-PM-*b*-PLA Triblock Copolymers. For the purpose of mechanical testing and evaluation of TPE behavior, we targeted a triblock copolymer with hexagonally packed cylinders of PLA in a PM matrix. TPEs within hexagonally packed cylinders typically display impressive recoveries and high elongations at break.[9] Successful synthesis of LML(7.8−29−7.8) was achieved by utilizing molecular sieves during the lactide triblock polymerization to eliminate water and by performing multiple precipitations of the product to remove residual HCl (see Experimental Section); the larger scale syntheses were not successful without these precautions. The final product was a rubbery solid with SEC traces and ^{1}H NMR spectra typical of the triblock copolymers previously

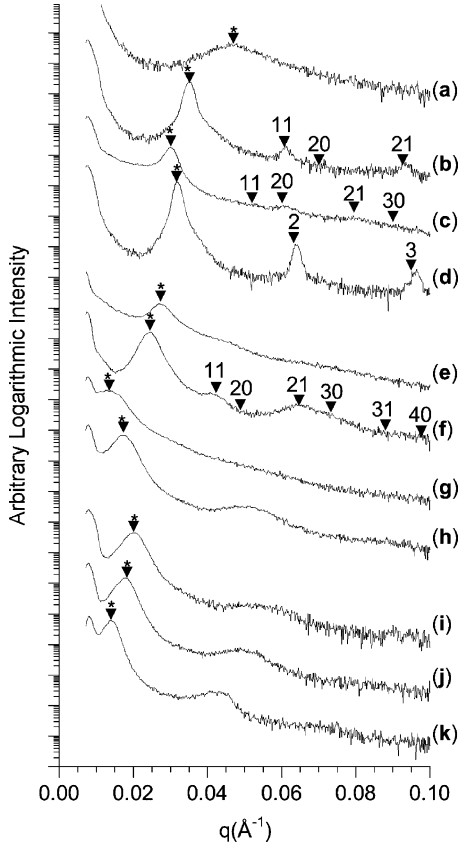

Figure 4. SAXS of all PLA-*b*-PM-*b*-PLA triblock copolymers at 80 °C. (▼) Peak positions calculated based on **q*** (marked with an asterisk) are labeled by their Miller indices (**hk** for the two-dimensional hexagonal lattice, **h** for the one-dimensional lamellar lattice). For samples with little or no lattice order, only **q*** is indicated. (a) LML(1.3−10−1.3), (b) LML(2.3−10−2.3), (c) LML(3.8−10−3.8), (d) LML(4.6−10−4.6), (e) LML(3.3−28−3.3), (f) LML(6.6−28−6.6), (g) LML(9.7−28−9.7), (h) LML(14−28−14) (This sample exhibits the ordered lamellar morphology above 140 °C.), (i) LML(10−43−10), (j) LML(15−43−15), (k) LML(23−43−23).

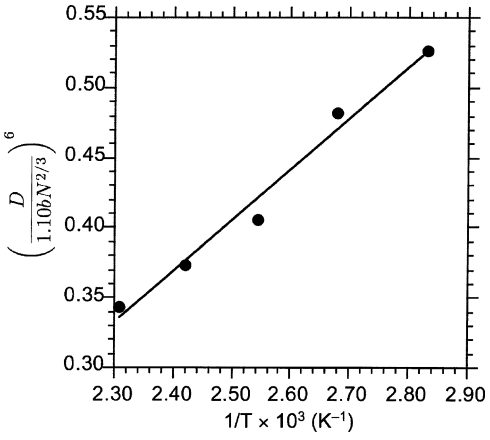

Figure 5. $(D/1.10bN^{2/3})^6$ vs $1/T \times 10^3$ for the lamellar LML(4.6−10−4.6). The line of best fit represents the estimate for χ: $\chi(T) = 364/T - 0.50$.

synthesized (see Experimental Section). DSC revealed two T_g's at −25 °C and 44 °C, and SAXS measurements were consistent with hexagonally packed cylinders of PLA in a matrix of PM (considering the relative fractions of PLA and PM).

The tensile properties of the PLA-*b*-PM-*b*-PLA triblock copolymer were characteristic, for the most part, of traditional TPEs. At low strains, a linear response was observed in the stress−strain curve for all of the trials. However, the Young's modulus observed (1.4 ± 0.3 MPa) was significantly reduced when compared to commercial polystyrene-*b*-polybutadiene-*b*-polystyrene TPEs (>6.0 MPa).[9] Representative stress−strain plots for the triblock copolymer pulled to ultimate tensile failure are shown in Figure 6. Beyond the low strain elastic region, the triblock copolymer shows yielding behavior indicative of a semicontinuous PLA phase dispersed in a PM matrix.[26] The ultimate tensile strength was 1.7 ± 0.1 MPa, which is also low compared to commercial polystyrene-*b*-polybutadiene-*b*-polystyrene TPEs (20−40 MPa). However, high elongations (960 ± 60%) were achieved for every trial. These ultimate elongations are comparable to those of commercial TPEs[9] and are higher than the largest elongations observed by the PLA-*b*-PI-*b*-PLA triblock copolymer series (650%) and the PLLA-*b*-PHB-*b*-PLLA triblock copolymer series (200%).[11,15]

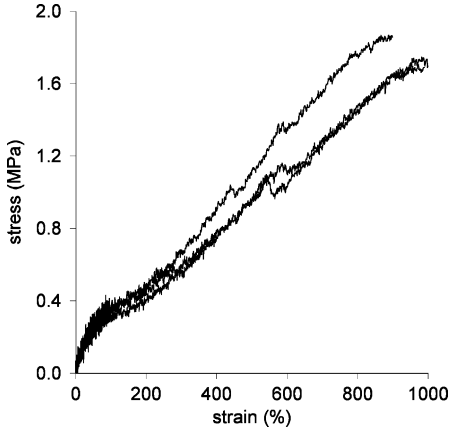

Figure 6. Three representative stress−strain curves for LML(7.8−29−7.8) pulled to ultimate failure.

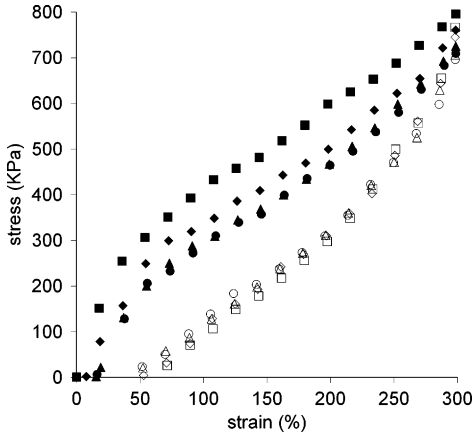

Figure 7. Four loading (filled symbols) and unloading (open symbols) cycles for LML(7.8−29−7.8) pulled to 300% with 6 min delays between cycles: first cycle, squares; second cycle, diamonds; third cycle, triangles; fourth cycle, circles.

We investigated the recovery or "true elasticity" of the triblock copolymer by subjecting the sample to cycles of loading and unloading at a strain of 300%. The recovery was measured by observing the residual strain after a sample was unloaded. Residual strain was measured in two separate trials. First, a sample was subjected to consecutive cycles of loading and unloading, resulting in a residual strain of 30% after four cycles. Second, a separate sample was subjected to four cycles and allowed 6 min between each cycle for maximum recovery, resulting in a residual strain of only 16% after four cycles (Figure 7).[9] In both trials the residual strain increased with each cycle and then remained constant after the third cycle. This could be due to an alignment of the cylinders induced by the applied

strain; as a result, the aligned polymer would not fully recover.[11,27] Once this putative alignment was achieved, the subsequent cycles displayed identical stress−strain behavior (Figure 7, third and fourth cycles). The lack of complete recovery can also be explained by a slippage of trapped entanglements in the soft block during deformation.[9] This slippage results in a delay of the failure of the hard domains in the TPE, resulting in elongated samples. The overall recovery of the samples is affected because the slippage of chains is not instantaneously reversible.[9,11,28] Most likely, the lack of recovery displayed by LML(7.8−29−7.8) is the result of both induced alignment and slippage of the PM block.

A separate sample of LML(7.8−29−7.8) was pulled to 200%, released to zero strain, and immediately pulled to ultimate failure. Ultimate tensile failure was not observed as a result of the sample slipping out of the grips at 1100%, which can be viewed as a lower limit. This value is significantly higher than that of the samples that were pulled once to failure (Figure 6).

Conclusion

A series of all biorenewable ABA triblock copolymer TPEs with soft PM and hard PLA segments were obtained with varying composition and morphology. Synthesis involved the ring-opening polymerization of **M** by DEG and $ZnEt_2$, giving the difunctional macroinitiator HO−PM−OH, followed by the ring-opening polymerization of lactide to yield the desired PLA-*b*-PM-*b*-PLA triblock copolymer. We were able to control the molecular weights of HO−PM−OH by varying the **M**-to-initiator ratio. These HO−PM−OH materials were characterized by NMR spectroscopy, SEC and DSC, and then subsequently used as macroinitiators for D,L-lactide polymerization. Three series of triblock copolymers with varied lactide composition were obtained. SEC traces of all of the samples showed unimodal signals and a gradual shift to the high molecular weight region when the PLA block length increased. Microphase separation of the blocks was confirmed by SAXS. Tensile measurements demonstrated impressive elongations and elastomeric properties of the PLA-*b*-PM-*b*-PLA TPEs. These results demonstrate that PLA-*b*-PM-*b*-PLA triblock copolymers are potentially suitable for numerous applications in the biomedical and pharmaceutical fields.

Acknowledgment. This work was supported primarily by the MRSEC program of the National Science Foundation under Award Number DMR-0212302. Acknowledgment is made to the donors of the American Chemical Society Petroleum Research Fund for partial support of this research. We also acknowledge the National Science Foundation (Grant No. CHE-9975357) and Cargill, Inc. for partial support of this work.

Supporting Information Available. Representative kinetic data for the decay of the absorbance of the peak at 1048 cm^{-1}. This material is available free of charge via the Internet at http://pubs.acs.org.

References and Notes

(1) Vert, M.; Schwach, G.; Engel, R.; Coudane, J. *J. Controlled Release* **1998**, *53*, 85−92.
(2) Albertsson, A.-C.; Varma, I. K. *Biomacromolecules* **2003**, *4*, 1466−1486.
(3) Ikada, Y.; Tsuji, H. *Macromol. Rapid Commun.* **2000**, *21*, 117−132.
(4) Drumright, R. E.; Gruber, P. R.; Henton, D. E. *Adv. Mater.* **2000**, *12*, 1841−1846.
(5) Dechy-Cabaret, O.; Martin-Vaca, B.; Bourissou, D. *Chem. Rev.* **2004**, *104*, 6147−6176.
(6) For examples, see: (a) Martin, O.; Averous, L. *Polymer* **2001**, *42*, 6209−6219. (b) Bechtold, K.; Hillmyer, M. A.; Tolman, W. B. *Macromolecules* **2001**, *34*, 8641−8648. (c) Ljungberg, N.; Colombini, D.; Wesslen, B. *J. Appl. Polym. Sci.* **2005**, *96*, 992−1002.
(7) For examples, see: (a) Sheth, M.; Kumar, R. A.; Dave, V.; Gross, R. A.; McCarthy, S. P. *J. Appl. Polym. Sci.* **1997**, *66*, 1495−1505. (b) Wang, Y.; Hillmyer, M. A. *J. Polym. Sci., Part A: Polym. Chem.* **2001**, *39*, 2755−2766. (c) Ohkoshi, I.; Abe, H.; Doi, Y. *Polymer* **2000**, *41*, 5985−5992. (d) Anderson, K. S.; Hillmyer, M. A. *Polymer* **2004**, *45*, 8809−8823.
(8) For examples, see: (a) Hiljanen-Vainio, M.; Karjalainen, T.; Seppala, J. *J. Appl. Polym. Sci.* **1996**, *59*, 1281−1288. (b) Chen, X.; McCarthy, S. P.; Gross, R. A. *Macromolecules* **1997**, *30*, 4295−4301. (c) Simic, V.; Pensec, S.; Spassky, N. *Macromol. Symp.* **2000**, *153*, 109−121. (d) Slivniak, R.; Domb, A. J. *Biomacromolecules* **2005**, *6*, 1679−1688. (e) Ba, C.; Yang, J.; Hao, Q.; Liu, X.; Cao, A. *Biomacromolecules* **2003**, *4*, 1827−1834.
(9) Holden, G.; Legge, N. R.; Quirk, R. P.; Schroeder, H. E. *Thermoplastic Elastomers*, 2nd ed.; Hanser/Gardner: Cincinnati, OH, 1993.
(10) (a) Foss, R. P.; Jacobson, H. W.; Cripps, H. N.; Sharkey, W. H. *Macromolecules* **1976**, *9*, 373−374. (b) Foss, R. P.; Jacobson, H. W.; Cripps, H. N.; Sharkey, W. H. *Macromolecules* **1979**, *12*, 1210−1216.
(11) Frick, E. M.; Hillmyer, M. A. *Macromol. Rapid Commun.* **2000**, *21*, 1317−1322.
(12) Frick, E. M.; Zalusky, A. S.; Hillmyer, M. A. *Biomacromolecules* **2003**, *4*, 216−223.
(13) Huang, L.; Hu, J.; Lang, L.; Wang, X.; Zhang, P.; Jing, X.; Wang, X.; Chen, X.; Lelkes, P. I.; MacDiarmid, A. G.; Wei, Y. *Biomaterials* **2007**, *28*, 1741−1751.
(14) Sipos, L.; Zsuga, M.; Deak, G. *Macromol. Rapid Commun.* **1995**, *16*, 935−940.
(15) Hiki, S.; Miyamoto, M.; Kimura, Y. *Polymer* **2000**, *41*, 7369−7379.
(16) Zhang, Z.; Grijpma, D. W.; Feijen, J. *Macromol. Chem. Phys.* **2004**, *205*, 867−875.
(17) Stridsberg, K.; Albertsson, A.-C. *J. Polym. Sci., Part A: Polym. Chem.* **2000**, *38*, 1774−1784.
(18) Kricheldorf, H. R.; Rost, S. *Macromolecules* **2005**, *38*, 8220−8226.
(19) Wang, Y.; Ameer, G. A.; Sheppard, B. J.; Langer, R. *Nat. Biotechnol.* **2002**, *20*, 602−606.
(20) Zhang, D.; Hillmyer, M. A.; Tolman, W. B. *Biomacromolecules* **2005**, *6*, 2091−2095.
(21) (a) Zhang, D.; Hillmyer, M. A.; Tolman, W. B. *Macromolecules* **2004**, *37*, 8198−8200. (b) Zhang, D.; Xu, J.; Alcazar-Roman, L.; Greenman, L.; Cramer, C. J.; Hillmyer, M. A.; Tolman, W. B. *Macromolecules* **2004**, *37*, 5274−5281. (c) Gerhardt, W. W.; Noga, D. E.; Hardcastle, K. I.; Garcia, A. J.; Collard, D. M.; Weck, M. *Biomacromolecules* **2006**, *7*, 1735−1742.
(22) von Baeyer, A.; Villiger, V. *Ber. Dtsch. Chem. Ges.* **1899**, *32*, 3625−3633.
(23) Ishimori, M.; Tomoshige, T.; Tsuruta, T. *Makromol. Chem.* **1968**, *120*, 161−175.
(24) Williams, C. K.; Breyfogle, L. E.; Choi, S. K.; Nam, W.; Young, V. G.; Hillmyer, M. A.; Tolman, W. B., Jr. *J. Am. Chem. Soc.* **2003**, *125*, 11350−11359.
(25) (a) Semenov, A. N. *Sov. Phys. JETP* **1985**, *61*, 733. (b) Matsen, M. W.; Bates, F. S. *J. Polym. Sci., Part B: Polym. Phys.* **1997**, *35*, 945.
(26) See: Yu, J. M.; Teyssie, P.; Jerome, R. *Macromolecules* **1996**, *29*, 8362−8370.
(27) (a) Cohen, Y.; Albalak, R. J.; Dair, B. J.; Capel, M. S.; Thomas, E. L. *Macromolecules* **2000**, *33*, 6502−6516. (b) Honeker, C. C.; Thomas, E. L.; Albalak, R. J.; Hajduk, D. A.; Gruner, S. M.; Capel, M. C. *Macromolecules* **2000**, *33*, 9395−9406. (c) Honeker, C. C.; Thomas, E. L. *Macromolecules* **2000**, *33*, 9407−9417.
(28) For example, see: Mahanthappa, M. K.; Lim, L. S.; Hillmyer, M. A.; Bates, F. S. *Macromolecules* **2007**, *40*, 1585−1593.

BM700699G